Temporal Hierarchy of Gene Expression Mediated by Transcription Factor Binding Affinity and Activation Dynamics

Rong Gao, Ann M. Stock

Department of Biochemistry and Molecular Biology, Center for Advanced Biotechnology and Medicine, Rutgers University—Robert Wood Johnson Medical School, Piscataway, New Jersey, USA

ABSTRACT   Understanding cellular responses to environmental stimuli requires not only the knowledge of specific regulatory components but also the quantitative characterization of the magnitude and timing of regulatory events. The two-component system is one of the major prokaryotic signaling schemes and is the focus of extensive interest in quantitative modeling and investigation of signaling dynamics. Here we report how the binding affinity of the PhoB two-component response regulator (RR) to target promoters impacts the level and timing of expression of PhoB-regulated genes. Information content has often been used to assess the degree of conservation for transcription factor (TF)-binding sites. We show that increasing the information content of PhoB-binding sites in designed *phoA* promoters increased the binding affinity and that the binding affinity and concentration of phosphorylated PhoB (PhoB~P) together dictate the level and timing of expression of *phoA* promoter variants. For various PhoB-regulated promoters with distinct promoter architectures, expression levels appear not to be correlated with TF-binding affinities, in contrast to the intuitive and oversimplified assumption that promoters with higher affinity for a TF tend to have higher expression levels. However, the expression timing of the core set of PhoB-regulated genes correlates well with the binding affinity of PhoB~P to individual promoters and the temporal hierarchy of gene expression appears to be related to the function of gene products during the phosphate starvation response. Modulation of the information content and binding affinity of TF-binding sites may be a common strategy for temporal programming of the expression profile of RR-regulated genes.

IMPORTANCE   A single TF often orchestrates the expression of multiple genes in response to environmental stimuli. It is not clear how different TF-binding sites within the regulon dictate the expression profile. Our studies of *Escherichia coli* PhoB, a response regulator that controls expression of a core set of phosphate assimilation genes in response to phosphate starvation, showed that expression levels of PhoB-regulated genes are under sophisticated control and do not follow a simple correlation with the binding affinity of PhoB~P to individual promoters. However, the expression timing correlates with the PhoB-binding affinity and gene functions. Genes involved in direct P_i uptake contain high-affinity sites and are transcribed earlier than genes involved in phosphorus scavenging. This illustrates an elaborate mechanism of temporally programmed gene expression, even for nondevelopmental pathways.

Cells often respond to diverse environmental conditions by modulating the activity of transcription factors (TFs) that activate or repress the expression of target genes. When, where, and to what level each gene is expressed are crucial for appropriate responses and efficient adaptation. One of the basic mechanisms for controlling the magnitude and timing of gene expression is through *cis*-regulatory sequences that determine the TF occupancy of promoters (1–3). TF occupancy affects the recruitment of RNA polymerase (RNAP) for transcription output. In prokaryotes, promoter occupancy by a TF is largely controlled by the concentration of active TF and the interaction of active TF with specific binding sites within promoters, both of which collectively influence the timing and level of gene expression and coordinate an optimal expression pattern of different genes for environmental adaptation.

For genes activated by a TF, one common intuitive assumption is that the level and timing of gene expression correlate with the affinity of a TF for its target operator sequences within an individual promoter. Promoters with higher affinity for a TF tend to have higher TF occupancy that leads to higher probabilities of recruiting RNA polymerase (RNAP) for transcription initiation (2, 4). Additionally, the accumulation rate of active TF influences the time required for the concentration of active TF to reach the level for adequate promoter occupancy. Promoters with higher TF affinity require a lower concentration of active TF to achieve a given level of occupancy than do promoters with lower affinity and thus

are transcribed earlier. Different TF activation dynamics can adjust the timing difference between high-affinity and low-affinity promoters. These generalizations clearly represent an oversimplification of the transcription-regulatory mechanism in which many other factors, such as the positioning of TF-binding sites, interactions with other regulator proteins, and different RNAP recruiting efficiencies, can all influence the ultimate transcription output (1, 2, 4). Thus, it is necessary to determine how the level and timing of gene expression are correlated with the binding affinity of TFs and what the limitation and scope are for such generalized correlations. These issues are central to understanding how regulatory mechanisms are utilized by cells to coordinate gene expression for optimal responses to environmental stimuli.

Dependence of gene regulation on TF-binding affinity and activation dynamics is investigated here for the PhoB response regulator (RR) of *Escherichia coli*. The PhoB/PhoR regulatory system represents an archetype of the widely distributed prokaryotic two-component signal transduction scheme (5–8). PhoR, the histidine sensor kinase (HK), responds to limitation of environmental phosphate (P_i) concentrations by modulating the phosphorylation level of PhoB (8–10). Phosphorylated PhoB (PhoB~P) is the active form of the transcription regulator that binds to specific DNA sequences in target promoters, designated as Pho boxes, and interacts with the σ factor for RNA polymerase (RNAP) recruitment and gene activation (10, 11). For many bacterial TFs whose active form is not readily distinguishable from the inactive one *in vivo*, the exact cellular concentrations of the active form of TFs are usually difficult to track. In contrast, *in vivo* concentrations of the active RR, RR~P, can be quantified using Phos-tag gels (12). PhoB phosphorylation levels have been measured *in vivo* across a range of PhoB expression levels (9), which allows a quantitative assessment of how binding affinities affect gene expression levels at different PhoB~P concentrations.

A global binding profile of *E. coli* PhoB under P_i-depleted conditions has identified a wide variety of genes regulated by PhoB (13). Among them are several genes encoding proteins involved in phosphorus assimilation, including *phoBR*, *pstSCAB-phoU*, *phoE*, *ugpBAECQ*, *phoA*, and *phnCDEE′FGHIJKMNOP*. Genes with functions similar to the functions of these PhoB-activated genes are often found to be induced by phosphate starvation in other organisms as well (14–18). Expression of them enables cells to increase P_i uptake with more P_i-specific transporters and to utilize alternative phosphorus sources such as organophosphate and phosphonate (10). As phosphorus is an indispensable building block of cells, the expression level and timing of these genes may be coordinated to make efficient use of different phosphorus sources once the availability of the preferred inorganic orthophosphate is limited. Detailed expression analyses are required to evaluate the expression profiles of Pho regulon genes and assess the *cis*-regulatory elements that impact the expression of these genes.

Here we report that the expression timing of PhoB-regulated genes upon phosphate starvation correlates well with the binding affinity of PhoB~P for individual promoters whereas the expression levels are subject to more complex control. The information content (IC) in a 22-bp PhoB-binding site containing two tandem 11-bp repeats was found to have predictive power for relative levels of binding affinity, allowing design of *phoA* promoter variants with different affinities. For those *phoA* promoter alleles that contain base variations only within the PhoB-binding site, analyses in strains expressing PhoB constitutively showed a simple dependence of *phoA* expression on PhoB~P concentrations and the binding affinity. In contrast, for a core set of PhoB-regulated promoters with distinct −10 sequences and promoter architectures (i.e., with respect to the number, location, and orientation of PhoB-binding sites), the binding strength, specifically, the PhoB~P dissociation rate, shows little correlation with expression level even though the timing of expression follows the same order as the PhoB~P dissociation rates. Slower PhoB phosphorylation kinetics in the autoregulated wild-type (WT) strain cause larger timing differences between promoters, but the temporal order is maintained. Furthermore, the temporal hierarchy of gene expression appears to be related to the functions of the genes in this core set. Genes encoding alkaline phosphatase (AP) and phosphonate-utilizing proteins are expressed later and at higher PhoB~P levels during phosphate starvation than genes involved in direct P_i uptake. Our results demonstrate that the binding affinity characteristics of PhoB-binding sites are used to temporally program the expression profile of genes to match their functional roles in phosphate starvation responses.

RESULTS

The affinity of PhoB-binding sites depends on sequences of two 11-bp repeat elements. PhoB-binding sites have been well studied, and yet how variations in sequence affect binding affinities remains largely unknown, preventing a rational design of PhoB-binding site mutants to investigate how the TF-binding affinity impacts gene regulation. The PhoB-binding site is traditionally described as an 18-bp site that consists of two 7-bp direct repeats (5′-CTGTCAT-3′) separated by an AT-rich 4-bp spacer (10). Sequences of Pho boxes in both *phoB* and *phoA* promoters display high similarity to this consensus sequence, even though a considerably lower affinity for PhoB~P was observed for the *phoA* promoter (Fig. 1A; see also Fig. S1 in the supplemental material). This suggests that additional sequence features may contribute to the Pho box affinity. The structure of a PhoB-DNA complex (19) reveals two 11-bp tandem repeats contacted by PhoB, with each repeat containing a TGTCA tract involved in major groove contacts flanked by AT-rich bases at positions of minor groove contacts (Fig. 1A; see also Fig. S1B). A 22-bp span of DNA, longer than the minimal 18-bp site, is covered by PhoB. The 4-bp extension is within the minor-groove-contacting region and shows a slight preference for A/T bases (Fig. 1A). Compared to the *phoB* promoter, the binding site within the *phoA* promoter contains exclusively G/C base pairs in this region as well as one G/C pair in the upstream minor-groove-contacting region. This may contribute to its low affinity because A/T-rich segments are suggested to narrow the minor groove and thus facilitate minor groove contacts (3, 20, 21). When all identified PhoB-binding sites were extended to 22 bp to reconstruct a position weight matrix (PWM), a much lower information content (IC), a score commonly used to evaluate the degree of conservation for transcription factor binding sites (22), was observed for *phoA*, indicating a match to the PWM that is weaker than that seen with *phoB*, consistent with its lower affinity.

To create *phoA* promoter variants with different PhoB~P affinities, substitutions were made in both the minor-groove-contacting and major-groove-contacting regions (Fig. 1A; see also Fig. S1B in the supplemental material). Keeping the TGTCA tract intact, G/C pairs were substituted with A/T pairs in the minor-groove-contacting region to generate *phoA*Hi, a construct with
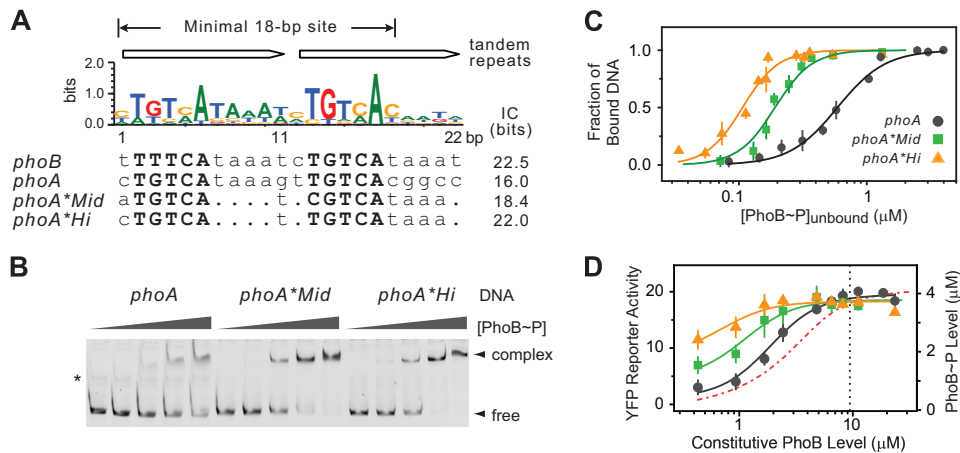
FIG 1 Dependence of YFP reporter activities on DNA-binding affinities of *phoA* variants. (A) Consensus and individual sequences of PhoB-binding sites. The sequence logo of a 22-bp site, including two tandem repeats, was generated from 21 sites (see Table S2 in the supplemental material for details). Bold letters highlight bases that are involved in accommodating the recognition helix in the major groove. Dots indicate unchanged bases among *phoA* variants. (B and C) *In vitro* binding of PhoB~P to DNA fragments containing the indicated Pho box variants. A representative EMSA (B) is shown for comparison of *phoA*, *phoA*Mid*, and *phoA*Hi*. Approximately 0.1 μM DNA fragments (~200 bp) containing the indicated Pho box variants were incubated with 0, 0.08, 0.24, 0.4, and 0.6 μM PhoB~P protein as described in Materials and Methods. An asterisk marks the position of a nonspecific DNA band. (C) Fractions of bound DNA were quantified from relative intensities of unbound free DNA bands to generate the binding curves shown. Solid lines represent curves fitted with a Hill equation. (D) Normalized YFP reporter activities of *phoA* promoter variants. RU1616 or RU1783 containing reporter plasmids pRG161 (*phoA*), pRG383-A9 (*phoA*Mid*), and pRG383-A6 (*phoA*Hi*) was used to measure promoter activities at different PhoB expression levels under P_i-depleted conditions. YFP reporter fluorescence was normalized to OD_{600}. Concentrations of PhoB~P (red dashed and dotted line) were derived from previous experiments based on PhoB expression levels (9). The vertical black dotted line indicates the WT expression level of PhoB under P_i-depleted conditions. Error bars represent standard deviations (SDs) of the results from at least three independent experiments; unseen error bars are smaller than the symbols.

greatly increased PhoB~P binding affinity, as shown by the results of electrophoretic mobility shift assays (EMSAs) (Fig. 1B and C and Table 1). While maintaining all A/T substitutions in the minor-groove-contacting region, a T-to-C base substitution was made within the highly conserved consensus TGTCA tract to generate *phoA*Mid*, a mutant with an intermediate affinity, lower than that of *phoA*Hi* and higher than that of the original *phoA* promoter, which contains a perfect TGTCA tract. Information content calculated from sequences of 22-bp sites correctly recapitulates the ranking of PhoB~P affinities for these three sites and may be useful for prediction of the relative affinities of other PhoB-binding sites.

Expression levels of *phoA* promoters correlate with both PhoB-binding affinity and PhoB~P concentrations. *phoA*, *phoA*Mid*, and *phoA*Hi* were fused to a promoterless yellow fluorescent protein (YFP) to assess the impact of binding affinity on expression levels. Analogous to *in vitro* experiments in which different PhoB~P concentrations were used to derive the full binding curve, YFP reporter activities were measured in strains with a range of *phoBR* expression levels controlled by IPTG (isopropyl-β-D-thiogalactopyranoside) (see Fig. S2A and Table S1 in the supplemental material). PhoB~P concentrations depend on total PhoB levels and can be derived from previous *in vivo* phosphory-

lation analyses (9). All three variants showed minimal reporter activities under P_i-replete conditions (data not shown), and significant YFP fluorescence above background was observed only under P_i-depleted conditions, where PhoB is phosphorylated (Fig. 1D).

At low concentrations of PhoB~P, the promoter activities of the three variants exhibited the same order as their binding affinities, with *phoA*Hi* displaying the highest level and *phoA* the lowest. Consistently, when the concentration of PhoB~P increased, promoter activity of *phoA*Hi* saturated first, followed by *phoA*Mid* and *phoA* (Fig. 1D). Transcription reporter activities could certainly be affected by factors other than the TF-binding affinity *in vivo*, but the ratio of promoter activity to the saturated level has often been associated with *in vivo* promoter occupancy, which is commonly used to generate binding curves for estimating *in vivo* dissociation constants (K_d) (see Fig. S2B in the supplemental material). Even though the exact K_d values differ for *in vivo* reporter assays and *in vitro* EMSAs, the relative K_d values match very well (Table 1). In both assays, *phoA* has a K_d value about 5-fold that of *phoA*Hi* whereas the *phoA*Mid* has a K_d value that is approximately 2-fold higher than that of *phoA*Hi*. This clearly demonstrates that the binding affinity of PhoB~P to its target promoters influences the transcription output. However, the transcription output also depends on the concentration of active TF. The wild-type (WT) strain expresses PhoB at a concentration of ~9 μM under P_i-depleted conditions, and even the weakly binding *phoA* promoter reaches the saturated-expression level at this concentration. Thus, despite their distinct binding affinities, all promoter variants have comparable activities at the fully induced level of WT PhoB (Fig. 1D).

Gene expression onset time correlates with PhoB-binding affinity for *phoA* variants. Aside from the expression levels of pro-

TABLE 1 Dissociation constants of *phoA* mutants[a]

DNA	K_d (μM) from EMSAs	K_d (μM) from *in vivo* reporter assays
phoA	0.59 (5.3×)	1.6 (5.0×)
phoA*Mid	0.19 (1.7×)	0.66 (2.1×)
phoA*Hi	0.11 (1.0×)	0.32 (1.0×)

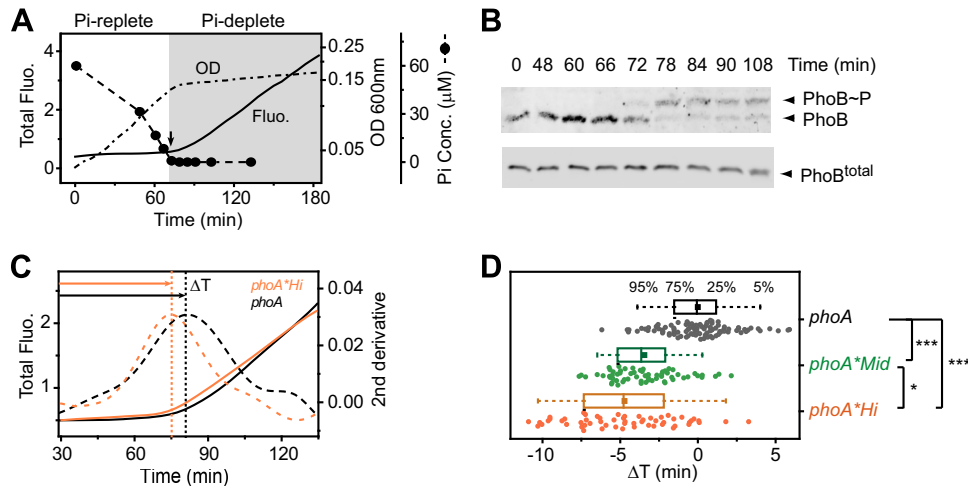[a] Numbers in parentheses are fold differences in K_d values.

FIG 2 Correlation between the timing of promoter activation and DNA-binding affinities of *phoA* variants. Temporal responses were analyzed in strain RU1616 with 150 μM IPTG, which has a steady PhoB expression level at ~8 μM, similar to the WT concentration of 9 μM seen under P_i-depleted conditions. (A) Activation of *phoA-yfp* upon phosphate starvation. The phosphate concentration (Pi Conc.) (solid circles), OD_{600} (dashed and dotted line), and total YFP fluorescence (Fluo.) (solid line) were monitored during growth. The arrow marks the first observed time point at which the P_i concentration became limited and fell below the documented 4 μM threshold for activation. The growth phase under P_i-depleted conditions is shaded gray. (B) Immunoblots showing *in vivo* phosphorylation levels of PhoB measured by the use of Phos-tag gels (upper panel) and total PhoB levels measured by the use of standard gels (lower panel). (C) Quantification of gene expression onset time. One representative analysis for each of the *phoA* and *phoA*hi* promoters is shown to illustrate the method. Dashed lines represent the second derivatives of cell fluorescence (solid lines), and dotted lines represent peak positions of the second derivatives that define the switch point of cellular fluorescence, marking the onset of reporter activation. (D) Distribution of onset time differences among *phoA* promoter variants. Individual data (solid circles) and box plots are shown with whiskers positioned at the 95th percentile and the 5th percentile. Solid squares indicate the mean values. Means of onset times were compared using one-way analysis of variance (ANOVA) and Tukey's *post hoc* test with P values as indicated (***, $P < 0.001$; *, $P < 0.05$). Sample sizes were as follows: for *phoA*, $n = 96$; for *phoA*Mid*, $n = 62$; and for *phoA*Hi*, $n = 58$.

moters, the timing of transcription may also be affected by Pho box affinity because the promoter occupancy by PhoB~P depends temporally on the dynamics of PhoB~P accumulation. When *E. coli* cells were grown in MOPS (morpholinepropanesulfonic acid) minimal media, phosphate was consumed and became limiting, followed by a change in the growth rate and in *phoA-yfp* activation (Fig. 2A). For the analyzed samples with a constant PhoB expression level close to the WT level (Fig. 2B; see also Table S1 in the supplemental material), the P_i concentration fell below the implicated activating threshold of 4 μM (10) between 66 and 72 min after inoculation into growth media whereas significant phosphorylation of PhoB was observed at 72 min and the phosphorylation reached a steady level 12 to 18 min later (Fig. 2A and B). Thus, any difference in transcription timing for *phoA* variants is expected to be less than the short time (12 to 18 min) required for PhoB~P saturation.

As shown in Fig. 2C, the peak of the second derivative of YFP fluorescence marks the switch point of cellular fluorescence, indicating the onset time of *yfp* expression. The timing of fluorescence onset is affected by the time required for transcription, translation, and maturation of the YFP reporter protein, all of which are greatly influenced by the growth rate and the metabolic state of cells in particular environments. Thus, relative timing in reference to the *phoA-yfp* reporter under identical phosphate starvation conditions is examined instead of the absolute timing of fluorescence onset. To quantify the difference of transcription timing, the second derivative peak is used to define the expression onset time of *phoA* promoter variants and the mean onset time of *phoA-yfp* was specified as a zero reference point. Because the phosphate consumption rate greatly influences the time when the P_i concentration reaches the activation threshold, any minuscule differ-

ences in growth rates among different cultures result in considerable variation in the activation onset time. Thus, gene expression onset times display a wide distribution (Fig. 2D). Nonetheless, the mean onset times of *phoA* variants differ significantly from each other. The *yfp* gene is expressed earliest under the control of *phoA*Hi* followed by *phoA*Mid* and *phoA*. An average of an ~5-min difference between *phoA*hi* and *phoA* in expression onset time was observed. Though small, this difference is not trivial in comparison to the short time required for PhoB~P to reach a steady-state concentration. Analysis of the distribution of gene expression onset times reveals a correlation of PhoB~P binding affinity with the timing of transcription activation.

The gene expression level and the onset time of PhoB-regulated promoters have different correlations with PhoB affinity. PhoB regulates a wide variety of genes with distinct roles in phosphorus assimilation. Many of these genes have more-complex promoter architectures than the well-characterized *phoA* promoter and often carry different numbers, locations, or orientations of PhoB-binding sites (Fig. 3A; see also Table S2 in the supplemental material). To assess the overall binding behavior of five selected promoters, entire promoter DNA fragments rather than individual sites were chosen for PhoB~P binding analyses using Bio-layer interferometry (BLI) (see Fig. S3). For simplicity, apparent dissociation rates (off-rates) were used to compare the binding affinities of PhoB~P to individual promoters (Fig. 3A and B). The PhoB-binding site within the *phoB* promoter has a lower PhoB~P off-rate than that of the *phoA* promoter, consistent with its higher affinity as shown in EMSA results (see Fig. S1). Again, information content predicted from the PWM matches the binding affinity of PhoB~P to promoters and the highest information content values of individual promoters correlate very well with the
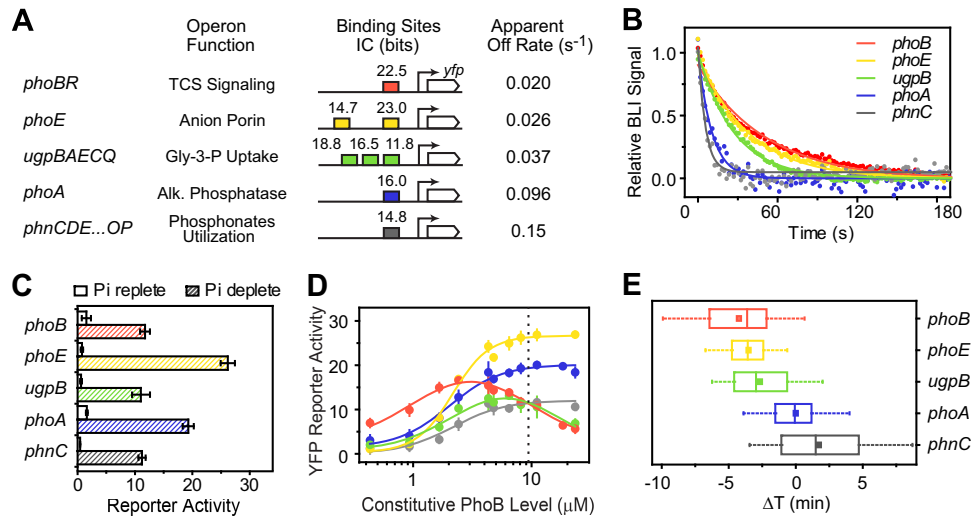
FIG 3 Effects of binding affinities on gene expression of PhoB-regulated promoters. (A) Details of PhoB-regulated promoters. The promoters tested were from five operons: *phoBR*, *phoE*, *ugpBAECQ*, *phoA*, and *phnCDEE'FGHIJKLMNOP*. Boxes illustrate the positions of PhoB-binding sites, and positions are proportional to their relative distances from the transcription start (see Text S1 in the supplemental material for detailed sequences and the positioning of Pho boxes). The numbers at the top indicate information content (IC) calculated from the 22-bp PWM. All five promoters are fused to identical *yfp* genes for expression analyses. Alk., alkaline. (B) Dissociation of PhoB-DNA complexes measured by Bio-layer interferometry (BLI). Data are fitted using single exponential decay (solid lines), and the apparent off rates are listed in panel A. (C to E) Expression level and timing of the indicated promoters. Reporter activities (C and D) are measured in RU1616, RU1618, and RU1783 with the following reporter plasmids: pJZG202 (*phoB*), pRG347 (*phoE*), pRG346 (*ugpB*), pRG161 (*phoA*), and pRG162 (*phnC*). Error bars represent standard deviations (SDs) of the results from at least four independent experiments. The vertical black dotted line in panel D indicates the WT expression level of PhoB under Pᵢ-depleted conditions. OD normalized reporter activities (C) and activation onset times (E) were measured at a PhoB expression level of ~8 μM. Box plots are plotted as described in the Fig. 2 legend. Means of onset times were compared using one-way ANOVA and Tukey's *post hoc* test with *P* values of each pair of <0.001 except for the following: for *phoB* and *ugpB*, *P* = 0.054; for *phoB* and *phoE*, *P* = 0.74; for *phoE* and *ugpB*, *P* = 0.69; and for *phoA* and *phnC*, *P* = 0.014. Sample sizes were as follows: for *phoB*, *n* = 61; for *phoE*, *n* = 34; for *ugpB*, *n* = 36; for *phoA*, *n* = 96; and for *phnC*, *n* = 36.

measured dissociation rates (Pearson coefficient $r = -0.9$, $P = 0.03$).

At a constant PhoB concentration of 8 μM, no apparent correlation between PhoB~P off-rates and promoter expression levels could be identified (Pearson coefficient $r = -0.06$, $P = 0.75$) (Fig. 3C). The reporter activities of *phoB*, *ugpB*, and *phnC* were similar to each other despite their distinct off-rates. The low-affinity Pho box within the *phoA* promoter has a high off-rate, but *phoA* displays the second-highest reporter activity. Moreover, these promoters display different dependencies of expression levels on PhoB concentrations (Fig. 3D). The reporter activities of *phoB* and *ugpB* decreased at high PhoB~P concentrations after the initial increase, suggesting repression of the promoter activity. Expression levels of *phoE*, *phoA*, and *phnC* increased monotonically along with PhoB levels, but the PhoB concentrations for half-maximal expression appeared similar and thus did not reflect the PhoB~P dissociation rates. These data suggest that for genes coregulated by PhoB~P, expression levels are not necessarily correlated with affinities of PhoB-binding sites within their promoters.

In contrast, expression onset times of these promoters correlate very well with their PhoB~P dissociation rates (Pearson coefficient $r = 0.61$, $P < 0.001$) (Fig. 3E). The *phnC* promoter, which has the highest off-rate for PhoB~P binding, indicative of low affinity, is expressed latest, while promoters with lower off-rates display earlier expression onset. Different gene expression onset times likely reflect differences in promoter occupancy by the PhoB protein as PhoB~P levels increase during phosphate starvation. Unlike gene expression levels that are modulated by many other factors in addition to promoter occupancy by the TF protein, the

timing of transcription may have a simple dependence on TF occupancy of the promoter, determined solely by the PhoB~P binding affinity and PhoB~P concentrations.

Gene expression onset time is correlated with PhoB affinity in WT cells. The temporal order of gene expression was observed in an engineered strain with a constant level of PhoB expression different from that observed in the WT strain, in which PhoB positively autoregulates its own expression and has a distinct dynamic pattern of PhoB~P accumulation. To investigate transcription timing differences in WT cells, we introduced a *phoA-cfp* reporter as an internal reference together with the promoter of interest that drives *yfp* expression (Fig. 4A). *phoA-cfp* was activated upon phosphate starvation, and the expression onset time of *phoA-cfp* was set as zero while the difference between cyan fluorescent protein (CFP) and YFP fluorescence onset times from the same culture was calculated to represent the expression timing difference. This allows evaluation of onset time differences independently of strain backgrounds, which reduces interference from growth rate variations between strains.

As shown in Fig. 4B, the expression onset times of *phoB*, *ugpB*, and *phoA* in both WT and constitutive strains displayed the same pattern as that shown in Fig. 3D. *phoB-yfp* was expressed the earliest followed by *ugpB* and *phoA*, correlating with their binding affinities. For strains containing *phoA-yfp*, the difference between CFP and YFP fluorescence onset times was not zero even though both *cfp* and *yfp* are behind the identical *phoA* promoter. The slightly earlier onset time of YFP fluorescence could be attributed to faster maturation of YFP than CFP (23) and to copy number differences of CFP and YFP reporter plasmids. Nevertheless, the
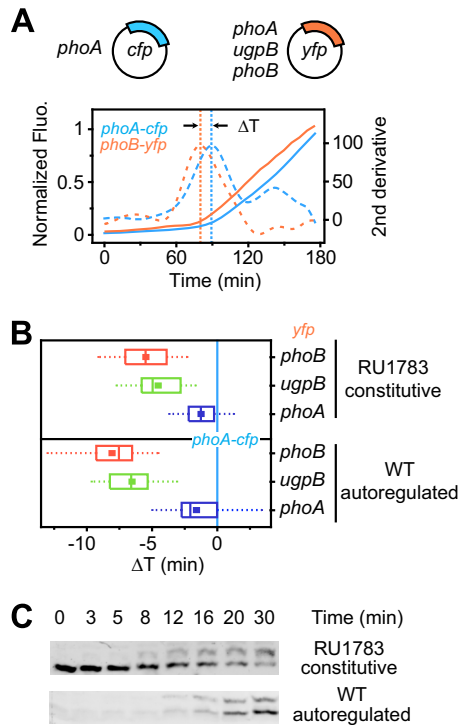
FIG 4 Gene expression onset times measured with an internal *phoA-cfp* reference. (A) Quantification of onset time differences with a dual-reporter system. Dashed lines represent the second derivatives of cell fluorescence (solid lines), and dotted lines represent peak positions of the second derivatives that define the onset of fluorescence reporter activation. (B) Distribution of onset time differences in both the WT strain (BW25113) and strain RU1783. Cells carrying pRG381 (*phoA-cfp*) and one of the three YFP reporter plasmids, pRG161 (*phoA*), pRG346 (*ugpB*), or pJZG202 (*phoB*), were assayed in the presence of 5 μM IPTG to maintain a PhoB concentration of 11 μM for RU1783. Box plots are plotted as described in the Fig. 2 legend. Means of onset times were compared using one-way ANOVA and Tukey's *post hoc* test. *P* values for onset time comparison of the same promoter between WT and RU1783 are as follows: for *phoA*, $P = 0.97$; for *ugpB*, $P = <0.001$; and for *phoB*, $P = <0.001$. Sample sizes were as follows: for *phoB*, $n = 39$ (RU1783) and 37 (WT); for *ugpB*, $n = 39$ (RU1783) and 40 (WT); and for *phoA*, $n = 39$ (RU1783) and 37 (WT). (C) Phosphorylation dynamics after the shift of bacteria to MOPS media containing an activating concentration (3 μM) of P_i.

expression onset times of *phoB*, *ugpB*, and *phoA* were significantly different from each other in both strains. Moreover, there was a significantly larger difference in expression onset time between *phoB-yfp* and *phoA-cfp* in the WT strain than in the constitutive RU1783 strain (Fig. 4B). The onset time difference of these two reporters represents the time required for the PhoB~P concentration to increase from the level sufficient for *phoB-yfp* activation to a higher level sufficient for *phoA-cfp* activation. A larger onset time difference suggests a slower increase in the PhoB~P level during phosphate starvation in the autoregulated WT strain than in the constitutive strain. Indeed, accumulation of PhoB~P was slower in the WT strain than in RU1783 as shown by a comparison of the phosphorylation kinetics of PhoB for the two strains immediately after the shift of bacteria to media containing an activating concentration (3 μM) of P_i (Fig. 4C). This is consistent with the discovery that positive autoregulation often causes a delay of response (24, 25).

The timing of expression of core genes in the PhoB regulon relates to their functions. The PhoB affinity of different genes

results in distinct expression times, but whether the expression timing relates to the gene function during phosphate starvation is unknown. Despite the largely different compositions of PhoB regulon genes in individual organisms, a core set of genes with common functions in phosphorus assimilation are often found to be induced upon phosphate starvation (14–18). These genes include *phoB* itself for regulation, anion- or P_i-specific outer membrane porin genes, high-affinity P_i-specific transporter (*pst*) genes for direct P_i uptake, and genes encoding alkaline phosphatase (AP) (e.g., *phoA*) and phosphonate utilization proteins (*phn*) for scavenging alternative phosphorus sources from organophosphate and phosphonate. Interestingly, the genes involved in utilizing organophosphorus sources, such as *phoA* and the *phn* genes, are all expressed late and contain weak PhoB-binding sites, while genes involved in direct P_i uptake and *phoB* itself contain high-affinity sites, suggesting a link between gene function and expression timing determined by the PhoB affinity level.

To explore whether the same link between gene function and the affinity of PhoB-binding sites is preserved in different organisms, information content of predicted PhoB-binding sites was examined in corresponding promoters across species. Information content calculated from the 22-bp PWM serves as a good indicator of PhoB-binding affinities, and PhoB proteins from different organisms have been shown to recognize similar DNA sequences (14, 26). Despite different gene arrangements or operon structures in some of the analyzed genomes, promoters controlling expression of *phoB* or P_i-uptake *pst* genes generally contain sites of higher information content than that seen with those expressing AP or phosphonate utilization *phn* genes (Fig. 5A). PhoB-binding sites are less conserved in more distantly related species, as indicated in the phylogenetic tree, and yet the pattern of higher-information-content sites in *phoB* and *pst* promoters persists. It appears that that affinity of PhoB-binding sites may be coupled to gene function to allow bacteria to program the timing of transcription for efficient use of the preferred phosphorus source, orthophosphate, before switching to alternative phosphorus sources.

DISCUSSION

Two-component signaling pathways are often described simply as static steps that eventually switch gene expression on or off. Growing numbers of reports have demonstrated sophisticated control of signaling dynamics along different steps of the pathway, and there is great interest in understanding the dynamic nature and mechanisms of regulating the expression profile (27). The results presented here reveal a temporal program of gene expression regulated by the PhoB/PhoR system and evaluate the correlation between PhoB binding affinities and the expression profiles of coregulated genes.

On the basis of a simple promoter occupancy model, it is often assumed that the expression level of a gene correlates with the TF-binding affinity because higher affinity results in higher occupancy of the promoter. Our results demonstrate that this assumption is not applicable for all promoters. For *phoA* promoter variants that differ only in the sequences of PhoB-binding sites, a correlation between gene expression levels and binding affinities was observed. Such a correlation is also observed in many other promoter mutants or synthetic promoter constructs that have different binding sites within otherwise identical promoter sequences (28, 29). However, in order for expression levels to reflect
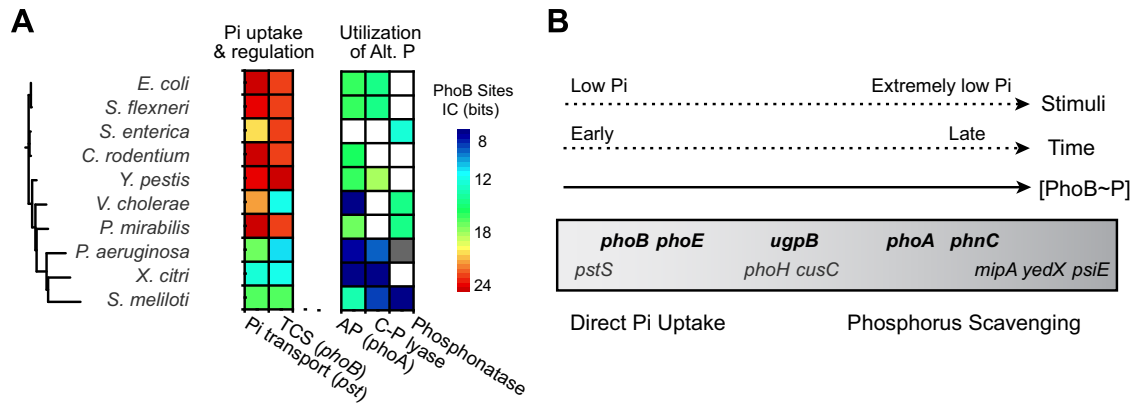
FIG 5 Relation between binding affinities and functions of core PhoB-regulated genes. (A) Information content of PhoB-binding sites from PhoB-regulated genes with distinct roles in phosphorus assimilation. The phylogenetic tree (left) was constructed using PhoB amino acid sequences from 10 species (amino acid identity values are indicated in parentheses): *Escherichia coli* K-12 (100%), *Shigella flexneri* 2a strain 301 (99%), *Salmonella enterica* serovar Typhimurium LT2 (96%), *Citrobacter rodentium* ICC168 (96%), *Yersinia pestis* KIM (90%), *Vibrio cholerae* O395 (81%), *Proteus mirabilis* HI4320 (79%), *Pseudomonas aeruginosa* PAO1 (62%), *Xanthomonas axonopodis* pv. *citri* strain 306 (59%), and *Sinorhizobium meliloti* 1021 (48%). PhoB-regulated genes were selected as described in Materials and Methods. For multiple PhoB sites within a single promoter or multiple promoters for genes having similar functions, only the highest information content is shown. Two different pathways are responsible for utilizing phosphonates, namely, the phosphonatase and C-P lyase pathways. Many bacteria contain only one pathway, and yet they all have sites of lower information content. White squares indicate the absence of a particular gene, while the gray square indicates the presence of the specific gene but a lack of PhoB sites. (B) Schematic representation of the relationship between PhoB-binding affinities and the order of gene expression. The gray gradient illustrates the decrease of binding affinities in PhoB-regulated genes that determines the PhoB~P level (solid line) required for sufficient promoter occupancy and gene activation. Differences in PhoB~P levels could reflect time after onset of P_i starvation or different stimulus intensities (dotted lines).

the binding affinities, the concentration of active TF must be below the level that saturates promoter occupancy. When the concentration of active TF is sufficiently high to saturate TF occupancy on either high- or low-affinity promoters, the effect of binding affinity on expression levels can be easily masked and differences in affinities will not be manifested in gene expression levels.

Unlike engineered variants, PhoB-regulated promoters do not share identical promoter architectures, regulation modes, or −10 sequences. Expression levels of these promoters showed no evident correlation with PhoB~P dissociation rates. Multiple factors may contribute to the absence of correlation. First, complex promoter architectures or alternative regulatory modes can complicate the regulation of gene expression (30, 31). Expression profiles of *ugpB* and *phoB* suggest additional repression mechanisms at high PhoB~P concentrations. Such repression causes a deviation of the expression level from that predicted by a simple occupancy model. An alternative overlapping promoter of the main *ugpB* promoter has been suggested to be inhibited by PhoB~P (32), while the repression mechanism for *phoB* has not been reported. Second, different promoters can recruit RNAP with different efficiencies. Mutations in the −10 region have been shown to alter the reporter activities of *phoE* and *pstS* promoters (33, 34). Thus, different sequences in the −10 regions of these promoters (see Table S2) may result in differences in the binding strength and recruitment efficiency of RNAP, enabling additional control of gene expression levels. Third, interaction with other regulators, such as the histone-like H-NS protein, could also interfere with TF occupancy and expression levels. It has been shown that gene ancestry and promoter architectures influence the silencing effects of histone-like nucleoid structuring (H-NS) on PhoP-regulated genes in *Salmonella* bacteria (35). Expression levels have been shown to be optimized for fitness (36), and cells have evolved many strategies to regulate expression levels. The binding affinity

is not the sole factor affecting gene expression and does not always correlate with expression levels if other factors are in play.

Different binding affinities give rise to the temporal order of expression for the core set of genes coregulated by PhoB. Similar mechanisms have been shown for the regulation of biofilm formation and sporulation by the Spo0A response regulator in *Bacillus subtilis* (37) and for virulence control by BvgA in *Bordetella* species (38), and several other TFs have been shown in both prokaryotes and eukaryotes (39–41). Most of these TFs are involved in developmental pathways that often progress at a time scale of hours or even days. PhoB-regulated promoters displayed a much lower timing difference of only a few minutes between early and late genes. This is in agreement with the high rate of PhoB phosphorylation because the timing of expression is limited by the dynamics of TF activation. Similarly, the *Salmonella enterica* PhoP protein is phosphorylated at a rate comparable to that seen with PhoB, and PhoP-regulated genes also show a timing difference of minutes (35). Any factor that alters the rate of accumulation of active TF, such as the positive feedback for expression of *phoB*, can further fine tune or change the temporal pattern of gene expression (42).

The temporal order of gene expression has been found to correlate with the functional order of the corresponding gene products along a cascade of regulatory events (43, 44). It is very common for genes along a linear metabolic pathway to have ordered binding affinities to a TF, which allows an optimized sequential activation of genes (44, 45). No apparent functional cascade had been associated with PhoB-regulated genes until this study identified a correlation between expression timing and gene functions. Early genes include *phoB* itself, to set the pace of the response, and other genes involved in P_i uptake, while late genes are involved in scavenging alternative phosphorus sources (Fig. 5B). Such temporal programming may represent a fundamental aspect of phosphorus utilization and appears well conserved across bacterial

species as indicated by the information content of PhoB sites in corresponding genes. A similar temporal order exists even for a completely different phosphate starvation pathway in budding yeast (41, 46). The gene encoding a high-affinity P_i transporter contains strong sites for the TF Pho4 and is expressed earlier than genes encoding phosphate-scavenging proteins. The temporal order of gene expression may not always have an apparent correlation with gene functions as shown by the *Salmonella* PhoP regulon (35). Aside from the core set of genes involved in phosphorus assimilation, many other genes without obvious roles in phosphorus utilization are also regulated by PhoB (13) and it remains to be investigated whether a similar link between gene function and expression timing exists for these genes.

For laboratory batch cultures of bacteria, the benefit of an ~5-min difference in the timing of gene expression upon initiation of phosphate starvation is unclear. This timing difference reflects the different PhoB~P levels required for activation of P_i uptake and scavenging genes. Perhaps important to some environmental scenarios, the PhoB~P levels also correspond to the strength of stimuli (Fig. 5B). Under conditions of extremely low P_i, PhoB is maximally phosphorylated to ensure the induction of all phosphate-responsive genes. Under conditions of less extremely low P_i, representing a weak stimulus for PhoB phosphorylation, increasing the expression of the P_i-specific transporter may allow sufficient P_i uptake from the environment without the necessity to commit resources to make alkaline phosphatases and phosphonate utilization proteins.

The temporal expression program of PhoB-regulated genes requires PhoB-binding sites with different affinities for PhoB~P. Our characterization of the PhoB-binding sites reveals a potential mechanism for tuning binding affinity. On the basis of the structure of the PhoB-DNA complex and the tandem symmetry, a 4-bp region flanking the conventional 18-bp PhoB-binding site is an integral part of a full PhoB-binding site and contributes to minor groove contacts by a wing of the winged-helix DNA-binding domain. Sequence changes within the 4-bp region can alter the binding affinity without changing the major-groove-contacting TGTCA tract that is important for binding specificity. Sequences are less conserved within this 4-bp region than in the rest of the 18-bp region. This highly variable region may represent the outcome of evolutionary selection for different binding affinities in different PhoB-regulated promoters to orchestrate the temporal program of gene expression.

MATERIALS AND METHODS

Strains, plasmids, and growth conditions. Strains and plasmids used in this study are listed in Table S3 in the supplemental material. DH5α and GM2929 were used for general cloning of plasmids, while all the strains used for *in vivo* assays were derived from BW25113. Because strain RU1616 does not express PhoB to higher levels, strain RU1783 was created by integration of pRG378 into the chromosome of RU1618 at the lambda phage attachment site using the reported recombination strategies (47). Reporter plasmids were constructed by inserting the PCR fragments containing corresponding promoters into pJZG146, which has a promoterless *yfp* gene. All reporters contained identical ribosome-binding sites. Details of strain and plasmid construction are described in Text S1. Bacteria were grown at 37°C in LB broth or in MOPS minimal media (48) with a 0.4% glucose and amino acid mix (40 $\mu g/ml$).

In vivo **assays for reporter, PhoB expression, and phosphorylation levels.** To achieve P_i depletion and induce phosphate starvation responses, cells from fresh P_i-replete (1 mM KH_2PO_4) MOPS precultures

were washed and inoculated in MOPS medium containing 50 μM KH_2PO_4. For the desired PhoB expression levels, different IPTG concentrations were used in precultures for protein induction and maintained in the media throughout the assay. For reporter assays, inoculated cultures were transferred to 96-well plates and continuously assayed for YFP fluorescence and optical density at 600 nm (OD_{600}) using a Varioskan plate reader (Thermo Scientific) with constant shaking. Similarly inoculated bulk cultures were grown for 3 to 4 h to measure PhoB expression and phosphorylation levels. As described previously (9), PhoB expression levels were measured using quantitative Western blot analyses with purified PhoB protein as the standard.

To examine the time-dependent responses, aliquots were removed at indicated time points to measure OD_{600}, P_i concentration, and PhoB phosphorylation. Bacteria were harvested, and the supernatant was frozen for later measurement of P_i concentrations. P_i concentrations were measured with the ascorbic acid-molybdate method (49). Cell pellets equal to approximately 0.3 OD · ml of cells were immediately resuspended in 55 μl 1× BugBuster reagent (Novagen) for lysis followed by denaturation with 18 μl 4× SDS loading buffer. All samples were immediately flash frozen in dry ice-ethanol and later analyzed using Phos-tag gels as previously described (9). In order to compare phosphorylation dynamics between the WT and RU1783 strains, a different protocol was used because it is difficult to determine the exact time of phosphate starvation in cultures with an initial P_i concentration of 50 μM. Instead, cells from P_i-replete cultures were washed with MOPS medium (30 to 50 μM P_i) two times and resuspended in MOPS medium (3 μM P_i). Aliquots were removed at different time points and analyzed for PhoB phosphorylation as described above.

Data processing of reporter profiles. Quantification of reporter activities and onset times depends on the identification of the switch point of cellular YFP fluorescence. To determine the switching time point of the fluorescence trace, the second-order local slopes of every five consecutive data points were computed to represent the second derivatives of the fluorescence levels. OD_{600} measurements were subject to some variations, while traces of total cellular fluorescence were smooth enough to calculate the derivatives (see Fig. S4 in the supplemental material). Thus, total fluorescence, instead of OD-normalized fluorescence, was used for derivative analyses. YFP expression onset time calculated from total fluorescence traces appears to have a distribution comparable to that calculated from OD normalized fluorescence traces (see Fig. S4).

The time point for the maximal second derivative value was chosen as the starting point, and the YFP fluorescence 90 min after the starting point was normalized to OD_{600} to represent the reporter activity. Because the exact peak of the second derivative does not always reside exactly at the experimental time point, the second derivatives were further differentiated to compute the point at which the third derivatives become zero, indicating the exact peaking point of the second derivatives. For reporter assays with the internal *phoA-cfp* reference, the difference between the YFP and CFP peaking points was used as the timing difference of gene expression. For assays lacking the internal reference, the time from an OD_{600} of 0.08 to the peaking point was computed as the YFP expression onset time and was further compared to the mean onset time of *phoA-yfp* to calculate the difference. OD_{600} measured in 96-well plates has a path length of less than 1 cm, and cells with an OD_{600} of 0.08 have already entered the log phase. The arbitrary choice of reference points at different OD_{600} levels within the log phase does not significantly alter the distribution of timing differences between promoters (data not shown).

Electrophoretic mobility shift assays. DNA fragments containing corresponding promoters were generated by PCR using 5'-fluorescein-labeled primers, and PCR products were purified with QIAquick columns (Qiagen). Detailed sequences of the probes and primers used to generate them are listed in Text S1 in the supplemental material. Purified PhoB protein (35 μM) was phosphorylated at room temperature in phosphorylation buffer (50 mM Tris [pH 7.4], 100 mM NaCl, 10 mM $MgCl_2$) with 50 mM phosphoramidate for at least 1.5 h. Phos-tag gel analyses confirmed that >90% of the PhoB protein was phosphorylated under this

condition. Phosphorylation buffer containing the same concentration of phosphoramidate was mixed with the phosphorylated PhoB sample to yield different concentrations of PhoB~P that were subsequently incubated with approximately 0.1 μM fluorescent DNA fragments in binding buffer (50 mM Tris [pH 7.6], 200 mM NaCl, 0.1 mg/ml bovine serum albumin [BSA], 2 mM MgCl$_2$, 1 mM dithiothreitol, 5% glycerol) at room temperature for 30 min. Nonfluorescent competitor DNA was added at a concentration of 15 μM using a previously annealed 27-bp double-stranded DNA (dsDNA) oligonucleotide unless specified otherwise. Samples were then electrophoresed on 12% Tris-borate-EDTA (TBE) gels at 130 volt for 50 min on ice. DNA bands were visualized by fluorescence imaging using a FluorChem Q system (Alpha Innotech) and quantified with ImageJ (NIH).

BLI assays. DNA-binding kinetics were studied with an Octet RED96 Bio-layer interferometry instrument (forteBio) in kinetic buffer composed of the following ingredients: 50 mM Tris (pH 7.4), 200 mM NaCl, 2 mM MgCl$_2$, 10 mM phosphoramidate, 0.1% BSA, and 0.02% Tween 20. PhoB was phosphorylated for 1.5 h and diluted to a final concentration of 0.3 μM. DNA fragments were generated using a biotinylated primer in a manner similar to that described for the EMSAs and were immobilized on streptavidin biosensor tips followed by collection of Bio-layer interferometry (BLI) signals upon PhoB~P association and subsequent dissociation into the blank kinetic buffer. Dissociation kinetic data were extracted to fit with a single exponential decay, while the full range of binding data were fitted with a 1:1 model of association and dissociation functions.

Calculation of information content. A total of 21 PhoB-binding sites that had been validated by *in vitro* binding experiments (see Table S2 in the supplemental material) were aligned to generate either the 18-bp or 22-bp PWM. Information content (IC) scores ($R_{sequence}$) of individual sites were calculated using Bioword (50) and are indicated in bits. To evaluate IC of PhoB-binding sites across species, genes with distinct phosphorus assimilation functions were selected based on predicted orthologs of *E. coli* genes from MicrobesOnline (51) or on the corresponding PhoB-regulon characterization in these species (14–18). DNA sequences 250 bp upstream of the translation start were searched using the 22-bp PWM to identify PhoB-binding sites and to calculate IC. For cases in which there were multiple sites predicted, the highest information content is reported in Fig. 5.

SUPPLEMENTAL MATERIAL

Supplemental material for this article may be found at http://mbio.asm.org/lookup/suppl/doi:10.1128/mBio.00686-15/-/DCSupplemental.

Text S1, DOCX file, 0.02 MB.
Figure S1, EPS file, 2.7 MB.
Figure S2, EPS file, 1.2 MB.
Figure S3, EPS file, 1.1 MB.
Figure S4, EPS file, 0.6 MB.
Table S1, DOC file, 0.04 MB.
Table S2, DOC file, 0.1 MB.
Table S3, DOC file, 0.1 MB.

REFERENCES

1. **Segal E, Widom J**. 2009. From DNA sequence to transcriptional behaviour: a quantitative approach. Nat Rev Genet **10**:443–456. http://dx.doi.org/10.1038/nrg2591.
2. **Bintu L, Buchler NE, Garcia HG, Gerland U, Hwa T, Kondev J, Phillips R**. 2005. Transcriptional regulation by the numbers: models. Curr Opin Genet Dev **15**:116–124. http://dx.doi.org/10.1016/j.gde.2005.02.007.
3. **Levo M, Segal E**. 2014. In pursuit of design principles of regulatory sequences. Nat Rev Genet **15**:453–468. http://dx.doi.org/10.1038/nrg3684.
4. **Browning DF, Busby SJ**. 2004. The regulation of bacterial transcription

5. **Gao R, Stock AM**. 2009. Biological insights from structures of two-component proteins. Annu Rev Microbiol **63**:133–154. http://dx.doi.org/10.1146/annurev.micro.091208.073214.
6. **Gao R, Stock AM**. 2010. Molecular strategies for phosphorylation-mediated regulation of response regulator activity. Curr Opin Microbiol **13**:160–167. http://dx.doi.org/10.1016/j.mib.2009.12.009.
7. **Capra EJ, Laub MT**. 2012. Evolution of two-component signal transduction systems. Annu Rev Microbiol **66**:325–347. http://dx.doi.org/10.1146/annurev-micro-092611-150039.
8. **Hsieh YJ, Wanner BL**. 2010. Global regulation by the seven-component pi signaling system. Curr Opin Microbiol **13**:198–203. http://dx.doi.org/10.1016/j.mib.2010.01.014.
9. **Gao R, Stock AM**. 2013. Probing kinase and phosphatase activities of two-component systems *in vivo* with concentration-dependent phosphorylation profiling. Proc Natl Acad Sci U S A **110**:672–677. http://dx.doi.org/10.1073/pnas.1214587110.
10. **Wanner BL**. 1996. Phosphorus assimilation and control of the phosphate regulon, p 1357–1381. *In* Neidhardt FC, Curtiss R, III, Ingraham JL, Lin ECC, Low KB, Jr, Magasanik B, Reznikoff WS, Riley M, Schaechter M, Umbarger HE (ed), *Escherichia coli* and *Salmonella*. ASM Press, Washington, DC.
11. **Blanco AG, Canals A, Bernues J, Sola M, Coll M**. 2011. The structure of a transcription activation subcomplex reveals how σ^{70} is recruited to PhoB promoters. EMBO J **30**:3776–3785. http://dx.doi.org/10.1038/emboj.2011.271.
12. **Barbieri CM, Stock AM**. 2008. Universally applicable methods for monitoring response regulator aspartate phosphorylation both *in vitro* and *in vivo* using phos-tag-based reagents. Anal Biochem **376**:73–82. http://dx.doi.org/10.1016/j.ab.2008.02.004.
13. **Yang C, Huang TW, Wen SY, Chang CY, Tsai SF, Wu WF, Chang CH**. 2012. Genome-wide PhoB binding and gene expression profiles reveal the hierarchical gene regulatory network of phosphate starvation in *Escherichia coli*. PLoS One **7**:e47314. http://dx.doi.org/10.1371/journal.pone.0047314.
14. **Yuan ZC, Zaheer R, Morton R, Finan TM**. 2006. Genome prediction of PhoB regulated promoters in *Sinorhizobium meliloti* and twelve proteobacteria. Nucleic Acids Res **34**:2686–2697. http://dx.doi.org/10.1093/nar/gkl365.
15. **Scholten M, Janssen R, Bogaarts C, van Strien J, Tommassen J**. 1995. The pho regulon of *Shigella flexneri*. Mol Microbiol **15**:247–254. http://dx.doi.org/10.1111/j.1365-2958.1995.tb02239.x.
16. **Von Kruger WM, Lery LM, Soares MR, de Neves-Manta FS, e Silva B, Neves-Ferreira AG, Perales J, Bisch PM**. 2006. The phosphate-starvation response in *Vibrio cholerae* O1 and *phoB* mutant under proteomic analysis: disclosing functions involved in adaptation, survival and virulence. Proteomics **6**:1495–1511. http://dx.doi.org/10.1002/pmic.200500238.
17. **Cheng C, Wakefield MJ, Yang J, Tauschek M, Robins-Browne RM**. 2012. Genome-wide analysis of the Pho regulon in a *pstCA* mutant of *Citrobacter rodentium*. PLoS One **7**:e50682. http://dx.doi.org/10.1371/journal.pone.0050682.
18. **Bains M, Fernandez L, Hancock RE**. 2012. Phosphate starvation promotes swarming motility and cytotoxicity of *Pseudomonas aeruginosa*. Appl Environ Microbiol **78**:6762–6768. http://dx.doi.org/10.1128/AEM.01015-12.
19. **Blanco AG, Sola M, Gomis-Ruth FX, Coll M**. 2002. Tandem DNA recognition by PhoB, a two-component signal transduction transcriptional activator. Structure **10**:701–713. http://dx.doi.org/10.1016/S0969-2126(02)00761-X.
20. **Hancock SP, Ghane T, Cascio D, Rohs R, Di Felice R, Johnson RC**. 2013. Control of DNA minor groove width and Fis protein binding by the purine 2-amino group. Nucleic Acids Res **41**:6750–6760. http://dx.doi.org/10.1093/nar/gkt357.
21. **Rohs R, Jin X, West SM, Joshi R, Honig B, Mann RS**. 2010. Origins of specificity in protein-DNA recognition. Annu Rev Biochem **79**:233–269. http://dx.doi.org/10.1146/annurev-biochem-060408-091030.
22. **Schneider TD, Stormo GD, Gold L, Ehrenfeucht A**. 1986. Information content of binding sites on nucleotide sequences. J Mol Biol **188**:415–431. http://dx.doi.org/10.1016/0022-2836(86)90165-8.
23. **Gordon A, Colman-Lerner A, Chin TE, Benjamin KR, Yu RC, Brent R**. 2007. Single-cell quantification of molecules and rates using open-source

initiation. Nat Rev Microbiol **2**:57–65. http://dx.doi.org/10.1038/nrmicro787.

microscope-based cytometry. Nat Methods **4**:175–181. http://dx.doi.org/10.1038/nmeth1008.

24. **Mitrophanov AY, Groisman EA**. 2008. Positive feedback in cellular control systems. Bioessays **30**:542–555. http://dx.doi.org/10.1002/bies.20769.

25. **Hermsen R, Erickson DW, Hwa T**. 2011. Speed, sensitivity, and bistability in auto-activating signaling circuits. PLoS Comput Biol **7**:e1002265. http://dx.doi.org/10.1371/journal.pcbi.1002265.

26. **Krol E, Becker A**. 2004. Global transcriptional analysis of the phosphate starvation response in *Sinorhizobium meliloti* strains 1021 and 2011. Mol Genet Genomics **272**:1–17. http://dx.doi.org/10.1007/s00438-004-1030-8.

27. **Salazar ME, Laub MT**. 2015. Temporal and evolutionary dynamics of two-component signaling pathways. Curr Opin Microbiol **24**:7–14. http://dx.doi.org/10.1016/j.mib.2014.12.003.

28. **Sharon E, Kalma Y, Sharp A, Raveh-Sadka T, Levo M, Zeevi D, Keren L, Yakhini Z, Weinberger A, Segal E**. 2012. Inferring gene regulatory logic from high-throughput measurements of thousands of systematically designed promoters. Nat Biotechnol **30**:521–530. http://dx.doi.org/10.1038/nbt.2205.

29. **Rajkumar AS, Denervaud N, Maerkl SJ**. 2013. Mapping the fine structure of a eukaryotic promoter input-output function. Nat Genet **45**:1207–1215. http://dx.doi.org/10.1038/ng.2729.

30. **Zwir I, Latifi T, Perez JC, Huang H, Groisman EA**. 2012. The promoter architectural landscape of the *Salmonella* PhoP regulon. Mol Microbiol **84**:463–485. http://dx.doi.org/10.1111/j.1365-2958.2012.08036.x.

31. **Park DM, Kiley PJ**. 2014. The influence of repressor DNA binding site architecture on transcriptional control. mBio **5**:e01684-14. http://dx.doi.org/10.1128/mBio.01684-14.

32. **Kasahara M, Makino K, Amemura M, Nakata A, Shinagawa H**. 1991. Dual regulation of the *ugp* operon by phosphate and carbon starvation at two interspaced promoters. J Bacteriol **173**:549–558.

33. **Scholten M, Tommassen J**. 1994. Effect of mutations in the −10 region of the *phoE* promoter in *Escherichia coli* on regulation of gene expression. Mol Gen Genet **245**:218–223.

34. **Makino K, Amemura M, Kawamoto T, Kimura S, Shinagawa H, Nakata A, Suzuki M**. 1996. DNA binding of PhoB and its interaction with RNA polymerase. J Mol Biol **259**:15–26.

35. **Zwir I, Yeo WS, Shin D, Latifi T, Huang H, Groisman EA**. 2014. Bacterial nucleoid-associated protein uncouples transcription levels from transcription timing. mBio **5**:e01485-14. http://dx.doi.org/10.1128/mBio.01485-14.

36. **Gao R, Stock AM**. 2013. Evolutionary tuning of protein expression levels of a positively autoregulated two-component system. PLoS Genet **9**:e1003927. http://dx.doi.org/10.1371/journal.pgen.1003927.

37. **Fujita M, Gonzalez-Pastor JE, Losick R**. 2005. High- and low-threshold genes in the Spo0A regulon of *Bacillus subtilis*. J Bacteriol **187**:1357–1368. http://dx.doi.org/10.1128/JB.187.4.1357-1368.2005.

38. **Williams CL, Cotter PA**. 2007. Autoregulation is essential for precise temporal and steady-state regulation by the *Bordetella* BvgAS phosphorelay. J Bacteriol **189**:1974–1982. http://dx.doi.org/10.1128/JB.01684-06.

39. **Ronen M, Rosenberg R, Shraiman BI, Alon U**. 2002. Assigning numbers to the arrows: parameterizing a gene regulation network by using accurate expression kinetics. Proc Natl Acad Sci U S A **99**:10555–10560. http://dx.doi.org/10.1073/pnas.152046799.

40. **Rowan S, Siggers T, Lachke SA, Yue Y, Bulyk ML, Maas RL**. 2010. Precise temporal control of the eye regulatory gene Pax6 via enhancer-binding site affinity. Genes Dev **24**:980–985. http://dx.doi.org/10.1101/gad.1890410.

41. **Lam FH, Steger DJ, O'Shea EK**. 2008. Chromatin decouples promoter threshold from dynamic range. Nature **453**:246–250. http://dx.doi.org/10.1038/nature06867.

42. **Levine JH, Fontes ME, Dworkin J, Elowitz MB**. 2012. Pulsed feedback defers cellular differentiation. PLoS Biol **10**:e1001252. http://dx.doi.org/10.1371/journal.pbio.1001252.

43. **Kalir S, McClure J, Pabbaraju K, Southward C, Ronen M, Leibler S, Surette MG, Alon U**. 2001. Ordering genes in a flagella pathway by analysis of expression kinetics from living bacteria. Science **292**:2080–2083. http://dx.doi.org/10.1126/science.1058758.

44. **Zaslaver A, Mayo AE, Rosenberg R, Bashkin P, Sberro H, Tsalyuk M, Surette MG, Alon U**. 2004. Just-in-time transcription program in metabolic pathways. Nat Genet **36**:486–491. http://dx.doi.org/10.1038/ng1348.

45. **Chechik G, Oh E, Rando O, Weissman J, Regev A, Koller D**. 2008. Activity motifs reveal principles of timing in transcriptional control of the yeast metabolic network. Nat Biotechnol **26**:1251–1259. http://dx.doi.org/10.1038/nbt.1499.

46. **Springer M, Wykoff DD, Miller N, O'Shea EK**. 2003. Partially phosphorylated Pho4 activates transcription of a subset of phosphate-responsive genes. PLoS Biol **1**:E28. http://dx.doi.org/10.1371/journal.pbio.0000028.

47. **Haldimann A, Wanner BL**. 2001. Conditional-replication, integration, excision, and retrieval plasmid-host systems for gene structure-function studies of bacteria. J Bacteriol **183**:6384–6393. http://dx.doi.org/10.1128/JB.183.21.6384-6393.2001.

48. **Neidhardt FC, Bloch PL, Smith DF**. 1974. Culture medium for enterobacteria. J Bacteriol **119**:736–747.

49. **Chen PS, Toribara TY, Warner H**. 1956. Microdetermination of phosphorus. Anal Chem **28**:1756–1758.

50. **Anzaldi LJ, Munoz-Fernandez D, Erill I**. 2012. BioWord: a sequence manipulation suite for Microsoft word. BMC Bioinformatics **13**:124. http://dx.doi.org/10.1186/1471-2105-13-124.

51. **Dehal PS, Joachimiak MP, Price MN, Bates JT, Baumohl JK, Chivian D, Friedland GD, Huang KH, Keller K, Novichkov PS, Dubchak IL, Alm EJ, Arkin AP**. 2010. MicrobesOnline: an integrated portal for comparative and functional genomics. Nucleic Acids Res **38**:D396–D400. http://dx.doi.org/10.1093/nar/gkp919.